

RSC Advances



This is an *Accepted Manuscript*, which has been through the Royal Society of Chemistry peer review process and has been accepted for publication.

Accepted Manuscripts are published online shortly after acceptance, before technical editing, formatting and proof reading. Using this free service, authors can make their results available to the community, in citable form, before we publish the edited article. This *Accepted Manuscript* will be replaced by the edited, formatted and paginated article as soon as this is available.

You can find more information about *Accepted Manuscripts* in the [Information for Authors](#).

Please note that technical editing may introduce minor changes to the text and/or graphics, which may alter content. The journal's standard [Terms & Conditions](#) and the [Ethical guidelines](#) still apply. In no event shall the Royal Society of Chemistry be held responsible for any errors or omissions in this *Accepted Manuscript* or any consequences arising from the use of any information it contains.



Journal Name

ARTICLE

Protein mediated textile dye filtration using graphene oxide-polysulfone composite membranes

V.R.S.S. Mokkaḡatı^a, Derya Yuksel. Koseoglu Imer^{b,c}, Nurmıray Yılmaz^d, Volkan Ozguz^a, İsmail Koyuncu^{b,c}

Received 00th January 20xx,
Accepted 00th January 20xx

DOI: 10.1039/x0xx00000x

www.rsc.org/

Here we report graphene oxide (GO) concentration dependent protein binding (BSA) and dye filtration (RO-16) capabilities of polysulfone-GO composite membranes under different pH conditions (2, 7 and 10). The membranes were fabricated with different GO concentrations (1, 2, 4 and 8% w/w) and were successfully characterized for their physical and chemical properties, as well as for their performance ability. The best BSA binding and dye rejection rates were observed with 2% GO membrane at pH=10, which were 95% and 78.26% respectively, suggesting that 2% is the optimal concentration. Further, considering the fact that RO-16 dye is acidic friendly, contact time studies were carried out with 2% GO membranes at pH=2 and pH=10. It was realized that 2% GO-polysulfone membrane at pH=2 show the highest dye rejection rate with 87.4%, supporting the importance of contact time in filtration technology.

Introduction

Polymeric membranes are most widely used in filtration applications. Though they exist for decades with continuous development through time, they do attract some drawbacks like fouling, mechanical de-stability, roughness and high essential protein binding. Several studies have been carried out for various applications in order to retain one or more above mentioned characteristics of the polymeric membranes by making composites [1-7]. Till date it is still a challenge to produce a perfect membrane which possess all the above mentioned characteristics. Since the discovery of graphene [8, 9] there have been numerous studies related to its applications in almost all known fields of science. Though graphene has widely been studied for its electrical properties, transparency, flexibility and ease of production at large scales [10-15], it is graphene oxide (GO) when it comes to filtration. GO is hydrophilic in nature, easy to disperse in water and other solvents and facilitates functionalization. There are several methods to prepare GO [16-18].

Graphene oxide is generally prepared by Modified Hummer's method [19]. Its use for filtration studies has been explored by integration with different polymeric components like polysulfone (PSf), PVDF, PES [20-22], each enhancing one or more properties. Several studies have been reported on graphene oxide (GO) - polymer composite membranes which are related to their physical,

thermal properties and performance abilities [23-26], while few others are related to their applications like anti-fouling property, filtration and hydrophilicity [27-31]. While protein binding capability of GO integrated polymeric membranes has also been studied and reported [32,33], limited literature is available related to the filtration of dyes using GO composite membranes. Few other applications of graphene oxide-polymer composite membranes include biosensors, fuel cells and in electro-chemistry [34-36].

Most of the dyes used today are synthetic. These dyes are stable, having more complex aromatic structure that makes them difficult to biodegrade [37,38]. Several types of dyes are used in various industries like leather, rubber, plastics, pharmaceuticals, cosmetics and food industries for coloring respective products. The residues are discharged in to the environment which turns out to be hazardous [39,40]. Most of the environmental discharge consists of a combination of dyes instead of a single dye which makes it more complicated to remove as some dyes are positively charged and some are negatively charged. Hence combination of sorbents is also needed in order to remove these dyes. Several literature studies suggest the removal of different types of dyes using sugarcane bagasse [37], protonated waste biomass [41], Microorganisms [42], fungi [43] are among a few to mention.

BSA (Bovine Serum Albumin), a standard protein with numerous biochemical applications is known to interact effectively with different carbon nanomaterials (44) and also can serve as a protein glue if chemically modified (45). In this work we report the protein (Bovine Serum Albumin) mediated textile dye filtration capability of different concentrations of GO- PSf composite membranes. Initially, experiments were carried out with bare PSf and BSA coated membranes to study the dye filtration mechanism, however, UV spectroscopy results between the inlet and outlet concentrations showed non-significant results. Though PSf-GO composite

^a Nanotechnology Research and Application Center (SUNUM), Sabancı University, Orhanlı/Tuzla, İstanbul 34956, Turkey

^b Department of Environmental Engineering, İstanbul Technical University, 34469, İstanbul, Turkey

^c National Research Center on Membrane Technologies, İstanbul Technical University, 34469, İstanbul, Turkey

^d Nanoscience and Nanoengineering department, İstanbul Technical University, 34469, İstanbul, Turkey

† Electronic Supplementary Information (ESI) available: membrane characterization techniques. See DOI: 10.1039/x0xx00000x

membranes were previously fabricated and thoroughly studied for different applications, to our knowledge this is the first time where dye rejection studies are carried out with GO-PSf composite membranes using BSA as an intermediate. Addition of GO to bare PSf membranes highly alters the mechanical strength, contact angle, pore size, surface charge, roughness and Young's modulus and in turn creates an internal platform for BSA binding. The chemical structure and property of BSA to bind to both GO and RO-16 (Reactive Orange) textile dye makes it feasible for dye filtration. After fabrication and prior to testing for protein binding and dye filtration, the membranes were characterized for their physical and mechanical properties.

Experimental

Polysulfone (PSf) was purchased from BASF chemical company and polyvinylpyrrolidone (PVP) (Mw=35,000) from ISP (USA). N, N-methyl pyrrolidone (NMP) was purchased from Sigma and used as a solvent. Graphene Oxide (GO) was acquired from Graphene Supermarket Inc (USA). All chemicals in this study were used without further purification.

Fabrication of bare and graphene oxide nanocomposite membranes

For bare PSf membrane preparation, firstly PVP (6%, w/w) was added to NMP and was stirred until it was completely dissolved followed by adding PSf (16%, w/w) into this solution. The dope solution was stirred at room temperature in order to form a homogeneous mixture. For dope solutions with GO (GO-nanocomposite membranes), firstly four different concentrations of GO (1, 2, 4 and 8 w/w) were dispersed in the solvent (NMP) using an ultrasonication probe for 30 min, followed by adding PVP (6%, w/w) and PSf polymer (16%, w/w) as previously described. Prior to membrane casting the formed dope solutions were degassed using an ultrasonication bath. The dope solutions were casted using a casting knife with gap setting of 200 μm on a glass plate and casted with 100 mm/sec velocity using a lab scale casting machine (Cambridge, UK, Sheen automatic film applicator). The casting films were left for 10 sec for solvent evaporation followed by immediate immersion in a de-ionized water bath to obtain polymer precipitation. The membranes were stored in de-ionized water for 2 weeks.

Membrane characterization techniques

The membranes were characterized for permeability, contact angle, Scanning Electron Microscopy (SEM), mechanical properties, zeta potential and porosity (more details are provided in supplementary information).

Preparation of protein-coated membranes

For protein coating, 100-mL volume of protein solution having same concentration (100 mg/L) was prepared by adding BSA to phosphate buffer solution (0.05 mol/L, pH 6.2). Dead-end filtration cell with a magnetic stirring apparatus was used for coating process. Bare and GO nanocomposite flat-sheet membranes were fixed into the filtration cell and initially rinsed with distilled water under pressure (2 bar) for 1 h. Further, the protein solution was filtrated from the same membrane at 1 bar and the protein concentrations

in the inlet and permeate suspensions after filtration were measured to determine the coating efficiency. Concentrations of BSA solutions were determined by HachLange DR500 UV Spectrophotometer. Retention performances of protein were calculated by Eq. (1);

$$R = 1 - \frac{C_p}{C_f} \times 100\% \quad (1)$$

where,

R: protein rejection (%),

C_p: protein concentration at permeate (mg/L)

C_f: protein concentration at feed (mg/L)

Dye filtration

The dye filtration performances of bare and GO nanocomposite membranes coated with protein layer were studied with feed containing an azo reactive dye solution, 100 mg/L of Reactive Orange (RO-16). RO-16 was chosen since it is one of the most commonly used dyes in the textile industry throughout the world. It has a molecular weight of 617.53 g/mol. The dye shows a maximum absorbance at $\lambda_{\text{max}} = 496 \text{ nm}$.

Dye solution at constant concentration was prepared by dissolving 100 mg of the dye powder in 1 L volumetric flask of de-ionized water at room temperature.

The filtration experiments of RO-16 dye solution were carried out at 2 bar for 1 h using dead-end stirred filtration cell at room temperature. The flux profile over time was monitored online gravimetrically by Eq. (2):

$$J = \frac{V}{(A \cdot t)} \quad (2)$$

where V is the volume of permeate water (L), A is the active membrane area (m^2) and t is the permeation time (h).

Further, the feed and permeate samples were taken for color analysis.

Results and Discussion

Membrane characterization

The fabricated membranes were characterized for roughness, contact angle, pore size, Young's modulus, surface charge, Scanning Electron Microscopy (SEM) and Fourier Transform Infrared Spectroscopy (FTIR). Table 1 briefs some morphological and surface characterization results. The contact angle of bare PSf membrane was measured as 71° and after the introduction of GO the contact angles were measured to be 91.49° , 87.86° , 79.81° and 69.23° for 1, 2, 4 and 8% respectively. Zhao et al [46] fabricated PVDF nanocomposite membranes with GO nanosheets and realized that composite membranes have decreasing contact angles with increasing GO concentration. The decrease in contact angle (increase of hydrophilicity) was attributed to the large amount of oxygen-containing groups of GO which are dispersed on the membrane surface.

Addition of GO increases the pore size of bare PSf membrane which further increased with increasing GO concentrations, which is a general trend for nanocomposite membranes.

Table 1. Characterization values of the membranes

Membrane type	Roughness (RMS, nm)	Contact Angle ($^{\circ}$)	Average pore size (μm)	Young's modulus ($\times 10^7$ Pa)	Surface charge (mV at pH 6.2)	Permeability
Bare PSf	70	71.0 ± 6.5	0.038	1.13	-21.0	157
1.0GO-PSf	170	91.49 ± 4.6	0.047	1.105	-23.4	150
2.0GO-PSf	90	87.86 ± 5.7	0.054	1.58	-15.1	171
4.0GO-PSf	140	79.81 ± 4.8	0.071	3.145	-8.7	213
8.0GO-PSf	240	69.23 ± 3.4	0.127	3.78	-13.2	235

Characterization values of Mechanical strength and Young's modulus are also shown in Table 1. In comparison with bare PSf membrane Young's modulus of the composite membranes seems to have improved, especially with 4% GO-PSf and 8% GO-PSf membranes. Young's modulus is an intrinsic property under small elastic deformations. Unlike ultimate strength and ultimate strain, Young's modulus values only reflect the stress-strain behavior in the initial state of the loading process [47]. Thus, the obtained results highlight that the coexistence of an efficient GO dispersion and PSf/GO covalent interactions may lead to the development of PSf/GO composite membranes with better mechanical performance abilities. It has also been realized that the surface charge of nanocomposite membranes decreases with increasing GO concentrations.

Scanning Electron Microscopy (SEM)

The membranes were characterized by Scanning Electron Microscope (SEM). As seen in Figure 1A, bare PSf shows a typical dense top layer on the top followed by huge macrovoids. On the other hand GO membrane cross section images show that the macrovoids are replaced by a polymer matrix with noticeable changes (Figure 1 (B,C,D,E)).

GO as a hydrophilic additive can have an effect on the rate of exchange between solvent and non-solvent during phase inversion process where it can increase the de-mixing by enhancing thermodynamic instability (28). As a result the pores that are formed during the phase inversion could grow larger because of the stress that is being induced on the polymer surface which in turn could be due to the rapid solidification of the polymer (48). According to Hagen-Poiseuille relationship, under same pressure, membrane thickness and dynamic viscosity of larger pores lead to large water flux (49).

This phenomenon can also be well supported by the contact angle and surface roughness measurements briefed in Table 1. With increase in GO concentration the contact angle reduces which shows the increase in hydrophilicity of the membranes. Also as mentioned above, there is a fast exchange of solvent during the phase inversion and due to this there are some nodules which were formed on the polymer, ultimately resulting in the increase of surface roughness of the membranes with increasing GO concentration except for 2% and 4% [30].

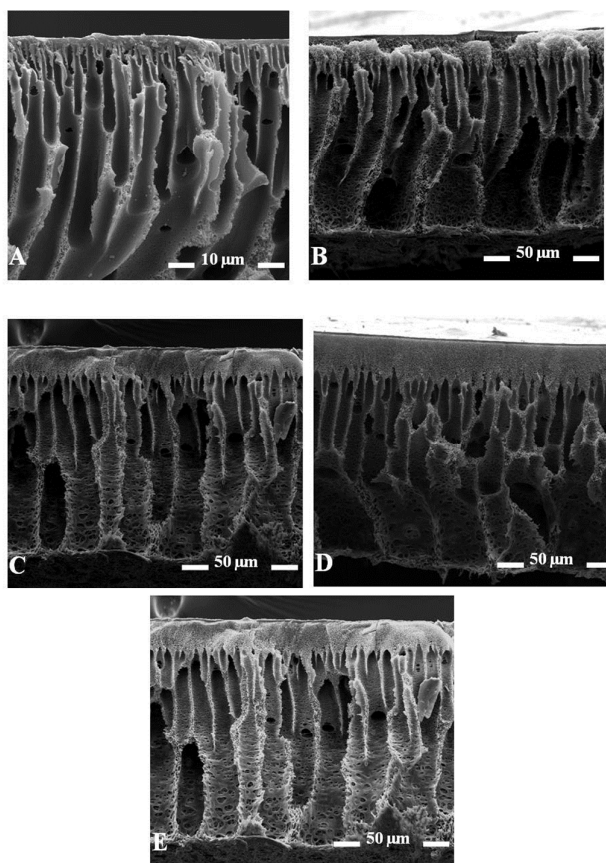


Fig. 1 SEM cross-section images of bare polysulfone and GO nanocomposite membranes. A: Bare PSf; B, C, D, E: 1%, 2%, 4% and 8% GO- PSf composite membranes respectively

From the SEM cross sectional images of 2% and 4% GO it can be observed that the dense top layer is well organized and relatively less rough (Table 1) compared to 1% and 8%. During the phase inversion process, water loving GO sheets tend to move to the top layer and settle there (this also has been proved by contact angle measurements). The dense top layer of 2% and 4% GO membranes show that the GO sheets organized themselves well with the available space. In comparison, 1% which had low concentration of GO sheets and 8% which had high concentration of GO sheets tend to stack and aggregate, increasing the surface roughness of the membrane. This low surface roughness has a role to play in the dye rejection process which will be explained in further sections.

Fourier Transform Infrared Spectroscopy (FTIR)

Prior to FTIR analysis the composite membranes were completely air dried. From the spectra shown in Figure 2 it can be observed that the peak intensity at 3340 cm^{-1} and 1712 cm^{-1} increases with the increase in GO concentration. These are characteristic peaks of GO and it can be realized that GO is well dispersed. The band at 1712 cm^{-1} is attributed to C=O [50]. The broad band between 3000 cm^{-1} and 3650 cm^{-1} attributes to O-H functional group stretching from graphene oxide surface. The absorption band of PSf spectrum at 1293 cm^{-1} corresponds to the O=S=O asymmetric stretching while the peak at 1148 cm^{-1} corresponds to symmetric stretching of O=S=O [30]. The weak peaks between 2850 cm^{-1} and 3200 cm^{-1} correspond to aliphatic and aromatic groups. The absorption band at 1241 cm^{-1} is attributed to asymmetric stretching of C-O-C group [30].

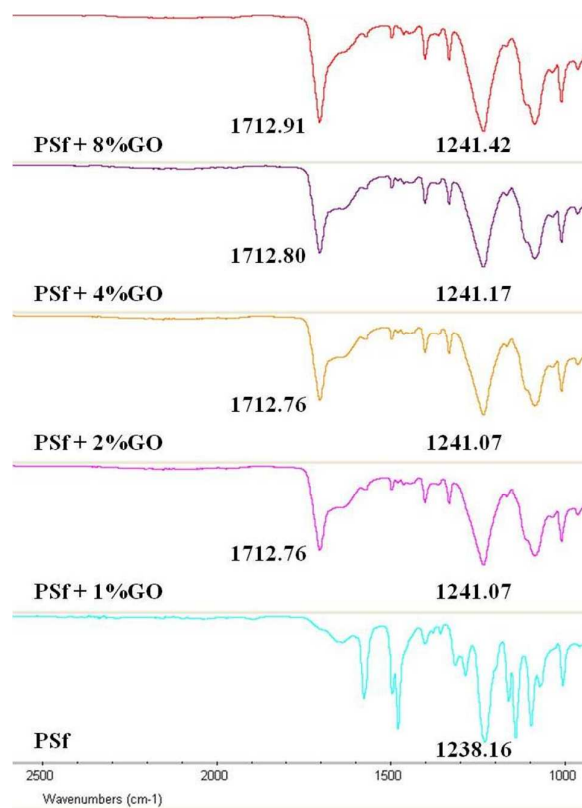


Fig. 2 FTIR spectra of polysulfone and different PSf + GO composite membranes

Permeability

Permeability tests were carried out using these membranes and the results are represented in Figure 3. The permeability of bare PSf membrane was found to be $154 \pm 15\text{ L/m}^2\cdot\text{h}\cdot\text{bar}$, where after GO introduction the permeability values were measured to be $150 \pm 20\text{ L/m}^2\cdot\text{h}\cdot\text{bar}$, $171 \pm 14\text{ L/m}^2\cdot\text{h}\cdot\text{bar}$, $213 \pm 17\text{ L/m}^2\cdot\text{h}\cdot\text{bar}$ and $235 \pm 20\text{ L/m}^2\cdot\text{h}\cdot\text{bar}$ for 1%, 2% and 4% and 8% GO concentrations respectively. As seen in the graph there is no difference between bare PSf and 1% GO membranes but with further increase in GO concentrations, the permeabilities of the nanocomposite membranes increase. GO increases the pore size of the membranes (Table 1) and the permeabilities of the phase inverted membranes

are generally related to the porosity and pore size of the membranes. From Table 1, it is clearly evident that with increased GO concentration there is an increase in the pore size of the membranes, further increasing the permeability.

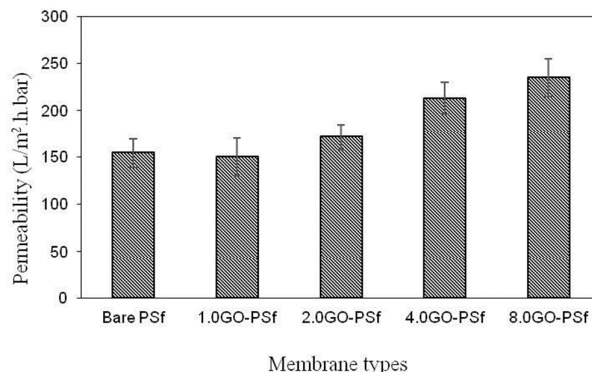


Fig. 3 Permeability graphs of bare PSf and Graphene oxide nanocomposite membranes

Membrane Flux

Membrane flux can be increased by increasing the hydrophilicity of the membrane. As seen in Table 1, with increasing GO concentration the contact angle reduces which means that the membranes are more hydrophilic (excluding bare PSf). Figure 4 shows the flux comparison between bare PSf and PSf-GO membranes of different GO concentrations. From the collected data and the trend it can be seen that 8% GO-PSf membrane has high flux compared to other membranes. So, the higher the hydrophilicity of the membranes the higher is the flux. In this case it has to be noted that the contact angles of bare PSf and 8.0% PSf-GO composite membranes are almost similar but 8.0% PSf-GO membranes has high flux.

Explanation: The hydrophilicity and flux are directly proportional however as can be seen from Table 1. the average pore size of 8.0% PSf-GO membranes is $0.124\text{ }\mu\text{m}$ compared to that of bare PSf which is $0.038\text{ }\mu\text{m}$, which directly contributes to the increase in flux.

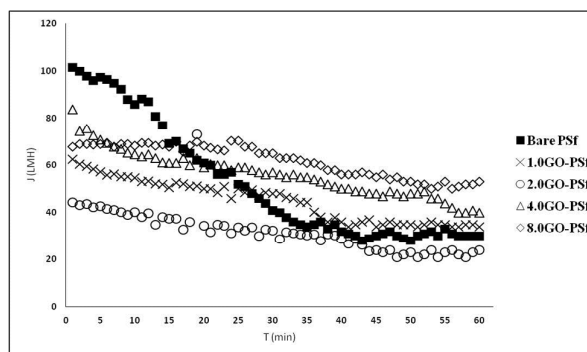


Fig. 4 Flux comparison between bare PSf and different PSf-GO composite membranes

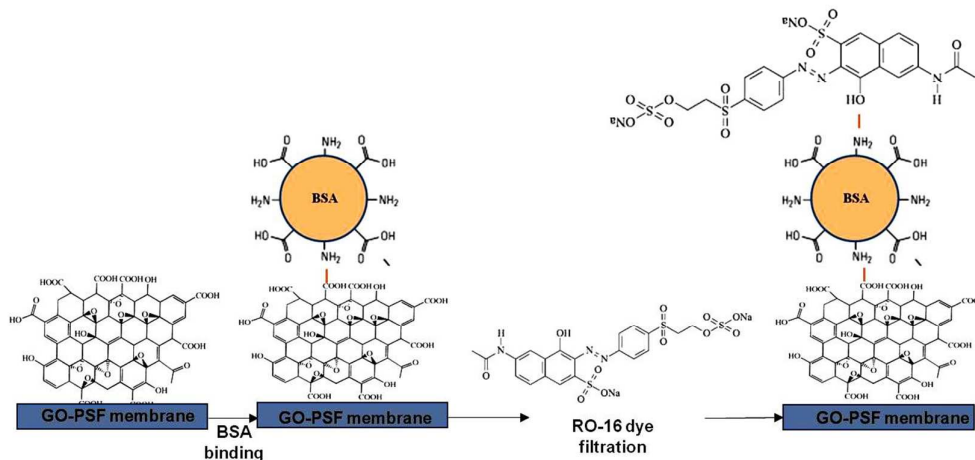


Fig. 5 Schematic illustration of protein coating onto membranes with dye attachment (*note: the figures are only a structural representation but not up to the scale*)

Dye filtration mechanism and performance of the membranes

Initially, experiments were carried out with bare PSf, 1, 2, 4 and 8% GO membranes (without BSA) for dye filtration. UV spectroscopy results revealed that these membranes are not effective enough to filter the dye molecules. Further, experiments were performed in two different stages:

1. Studying the protein binding ability of PSf + GO composite membranes and
2. Studying the dye rejection capability of protein bound GO + PSf membranes

These studies were carried out at acidic (2), neutral (7) and basic pH (10).

Bovine serum albumin (BSA), a standard protein was chosen as a protein of interest because of its numerous biochemical applications, low cost and stability. The preparation of BSA coated membranes was explained above, under sub-section “*preparation of protein coated membranes*”.

Dye sorption is mainly pH dependent and one of the most important factors that is to be considered for filtration mechanism. Experiments were carried out with all the membranes (bare PSf, 1, 2, 4, and 8% GO) at different pH values (2, 7 and 10). The pH of the solutions was optimized using HCl for acidic pH and NaOH for basic pH. Schematic representation of protein coating on to the composite membranes and dye binding to these protein coated membranes is shown in figure 5.

BSA binding

In our studies 2% GO membranes at pH=7 seem to be optimal for BSA binding. After permeability test results with different concentrations of GO + PSf membranes using BSA, UV spectroscopy results show that BSA binds to GO. The absorbance efficiency is calculated by:

$$\text{Absorption efficiency} = \frac{(\text{BSA inlet concentration} - \text{BSA outlet concentration})}{\text{BSA inlet concentration}} * 100$$

In our experiments, constant BSA concentration was used all through. BSA covalently binds to GO [51]. The amine groups of BSA bind to the carboxyl groups of GO (Figure 5).

As seen in Figure 6, the highest BSA binding efficiency was observed with 2% GO membranes at pH=7 which is about 95%, though bare PSf, 2% GO at pH=10 and 4% GO at pH=2 come close.

If we observe the trend with pH=7, after 2% GO the binding reduced only to increase again with 8% GO membrane. We presume that with the availability of more carboxyl groups, BSA naturally tends to bind further reaching a saturation level after 2%. With 4% GO there were enough free carboxyl groups available compared to amine groups of BSA (as mentioned above the BSA concentration is constant all through the experiment) and so the decrease in binding efficiency.

It was observed that BSA binding efficiency again increases with 8% GO, which we presume is due to the stacking of GO flakes on top of each other after certain concentration. Due to this stacking, there were relatively more and more bonding sites realized for BSA to bind to GO.

In the case of pH=10 after 2% we can observe a complete saturation and this can be attributed to the increase in surface charge. At higher pH, the zeta potential of the system is high, which means higher negative charge. As GO itself is negative and BSA is asymmetric (change in pH effects the protein form and structure), at high pH the electrostatic repulsion is also high.

In the case of pH=2 there was a decrease in trend after 4% which means that there was no stacking of GO sheets till this concentration. If we observe the above graph, pH=2 and pH=10 values of 8% GO membrane are almost similar in comparison to 4% GO membranes which shows a large difference. At pH=2 the system tends to be protonized due to H⁺ ions which means it attracts more asymmetrically charged BSA molecules.

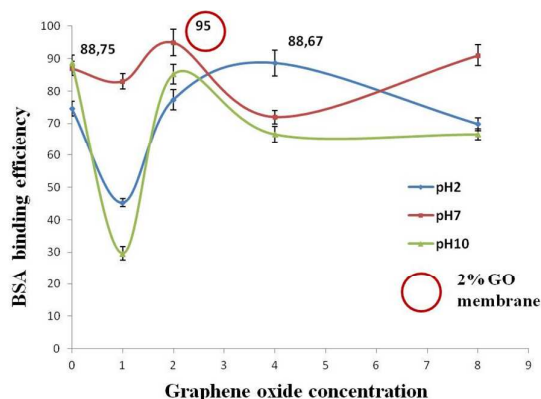


Fig. 6 Graphical representation of the calculated data for protein (BSA) binding

On the other hand BSA is non-uniformly charged at its primary structure, though it is more stable within the tertiary structure and these changes are caused due to the change in pH [52-54]. Due to this asymmetrical charge distribution it might be possible that BSA binds to GO (negative surface charge) at certain functional points (cationic) and repels itself from other locations. It has also been theoretically reported that only certain binding sites on BSA can be occupied by the dye molecules and the affinity varies from site to site due to the difference in polarity [55].

Due to this peculiar property of BSA it would be hard to achieve 100% binding even with significant increase in GO concentrations as the form of BSA also keeps changing with the change in pH [56].

Dye rejection

Permeability tests with the membranes of different GO concentrations with covalently bonded BSA were carried out. UV spectroscopy results suggest that the dye molecules were adsorbed on to the BSA (Figure 5). A constant RO-16 concentration was used in our experiments. The dye rejection rate is calculated by:

$$\text{Removal efficiency} = \frac{(\text{Dye inlet concentration} - \text{Dye outlet concentration})}{\text{Dye inlet concentration}} * 100$$

The calculated values and plotted graphs can be seen in Figure 7. In our studies maximum dye rejection was observed with 2% GO membranes at pH=10 though 2% GO at pH=2 comes closer. If we observe the trend at pH=2, after 2% the rejection rate gradually dropped. In case of pH=10 though the trend drops after pH=2, it draws a constant value for 4% and 8%.

Results at different pH's (2, 7 and 10) conclude that dye rejection rate increased till 2% further reducing with 4% and 8% which states that 2% GO concentration was optimal (Figure 7).

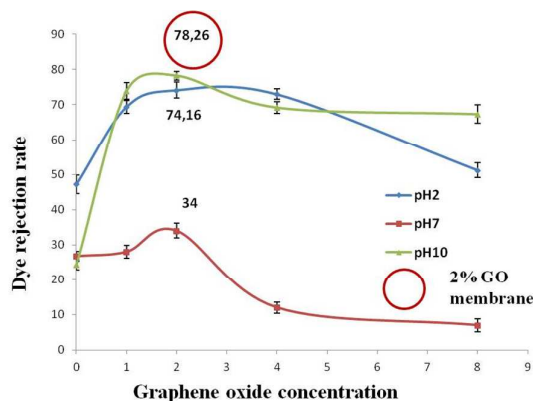


Fig. 7 Graphical representation of the calculated data for dye (RO-16) rejection

Note: Initial permeability tests on GO membranes with direct dye solution didn't show any significant variation with UV spectroscopy results. UV absorbance is same for the stock and the filtrate because the size of the RO-16 molecules was so small that they could easily pass through the intermolecular spaces within the membrane. By using GO-BSA bonded membranes, significant change in absorbance was observed.

In Figure 7 as seen in the graph, the rejection rate decreases after 2% GO. Certain parameters are to be taken in to consideration to explain this reduction phenomenon:

Size of the dye molecules in comparison to BSA: With increasing GO concentrations most of the free amine sites on BSA were occupied and along with this the intermolecular spacing was also blocked. BSA molecules are relatively huge compared to RO-16 molecules (BSA M.wt is approximately 66, 430 da as compared to that of RO-16 which is 617.53 g/mol) so the dye molecules were in fact blocked on the other side and this is valid only till 2% GO.

Further with the increase in GO concentrations there was an increase in BSA binding (except for 4%) which means the availability of more binding sites for RO-16 till 2%. With increase in GO concentration, we presume that the GO flakes stack on top of each other followed by BSA binding to them. This broadens the intermolecular spacing through which the dye molecules could easily permeate and because of this there was a reduction in dye rejection.

Anionic property of dye: RO-16 is anionic [57] so is GO which carries negative surface charge and due to coulombic repulsions the probability of GO binding to the dye molecules is very less. So, with increasing GO concentrations, dye molecule rejection is also supposed to increase but in fact after 2% GO concentration it reduces. As explained above, this is because GO flakes tend to stack on top of each other with increased concentrations and there by hindering the net negative surface charge and in turn broadening the intermolecular spacing which gives an easy access for the dye molecules to pass along with the permeate.

As observed, the change in the pH of the system affects the surface charge of the protein molecule and so the adsorption of charged dye molecules [58]. It has been reported that acidic pH is favourable for RO-16 removal [57]. A lower percentage of dye removal with

increase of GO concentrations is because of the presence of excess carboxyl groups which compete with the binding sites of the dye [59] resulting in electrostatic repulsion between anionic dye molecules and negatively charged GO sites. Table 2 summarizes the best performing membranes in terms of BSA binding and dye rejection.

Table 2. Comparison of membrane performance at different pH

pH	BSA (better performance) Binding efficiency	DYE (better performance) Removal efficiency
2	(4% GO) 88%	(2% GO) 74%
7	(2% GO) 95%	(2% GO) 34%
10	(control) 88%	(2% GO) 78%

As can be seen in Table 2, 2% GO membrane is found to be the best performing membrane in terms of BSA binding and dye rejection except for bare PSf at pH=10. Though bare PSf at pH=10 has 88% BSA binding ability, it fared quite poor in terms of dye rejection.

With the above experimental data we can conclude that 2% GO membranes are optimal in order to carry out high efficient filtration for textile dye RO-16. The maximum dye rejection capability observed was 78.26% at pH=10. Along with pH there are also certain other factors like initial concentration, agitation time and contact time which influence the filtration mechanism.

Effect of initial concentration: Initially when BSA or dye molecules were introduced in to the membrane there was a rapid adsorption further slowing down to be a gradual process, this is due to the availability of more free binding sites at the initial phase.

Agitation time: Agitation rate is also found to play an important role in the whole process as the increase in agitation rate decreases the film resistance and facilitates mass transfer.

Contact time: The most important of all is the contact time between the protein and the dye molecules. It has previously been reported that with increase in contact time the rejection capability increases [60-63]. During the adsorption process the dye molecules first have to overcome boundary layer effect and then adsorb on to the sorbent [58]. This process relatively takes a longer time.

Considering the above experimental results and facts, further experiments were carried out to study the effect of contact time between the protein and dye molecules. We have chosen 2% GO membrane based on its performance in terms of protein binding and dye rejection at difference pH values. Flux values were acquired for three different time intervals (45, 90 and 135 min).

The above presented data is reproducible and is not random. As explained in the above sections the correlation between bare PSf, 1, 2, 4 and 8% GO-PSf membranes, there has been either an increasing (roughness, pore size, Young's modulus) or decreasing (contact angle and surface charge) trends with increase in GO concentration, which is constant. This can be realized from the presented values and provided experimental evidence.

Contact time experiments

Taking in to consideration the importance of contact time between the protein and the dye molecules for higher dye rejection rate [60-63], contact time studies were carried out with the best performing membranes from the above experimental results.

Contact time experiments with 2% GO membranes at pH=2 and pH=10 were carried out in accordance with the above results. BSA solution at two different pH was prepared separately as mentioned in the previous section. Two 2% GO membranes were compressed for an hour at 2 bar before running the di-water flux. Firstly BSA solution at pH=2 was taken in the dead-end stirred cell filtration system (Steriltech), wait for 15 min for the solution to settle down, followed by the addition of dye solution. The BSA-dye solution was left under stirring for 45 min before acquiring first flux profile. After acquiring the first data the solution was left under continuous stirring for another 45 min (total 90 min) before acquiring the second flux profile, followed by third flux profile after 135 min. The same process was repeated for pH=10 BSA solution as well using a different 2% GO membrane.

The calculated values and plotted graph for contact time experiments are shown in Figure 8. As predicted, 2% GO at acidic conditions with 45 min contact time turned out to be most efficient in terms of dye rejection with 87.4% rejection rate. Previously it has also been stated that acidic conditions favour RO-16 removal [55]. As observed in Figure 8, the trend line after 45 min keeps reducing which shows that the contact time between the BSA and dye

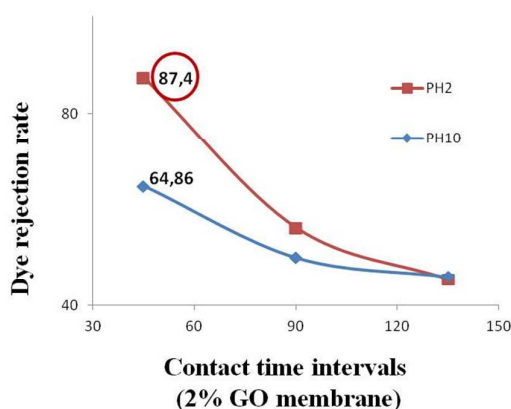


Fig. 8 Graphical representation of the calculated data for dye (RO-16) rejection after contact time studies

molecules turned out to be inefficient after 45 min. A valid reason for this decreasing trend line lies within BSA which will be further discussed in the next section. Table 3 briefs the comparison of final results in terms of dye rejection.

Table 3. Comparison of final results after contact time studies

pH	Time frame 45 min (dye removal efficiency)	Time frame 90 min (dye removal efficiency)	Time frame 135 min (dye removal efficiency)
2	87.4%	56.2%	45.45%
10	64.86%	50%	46%

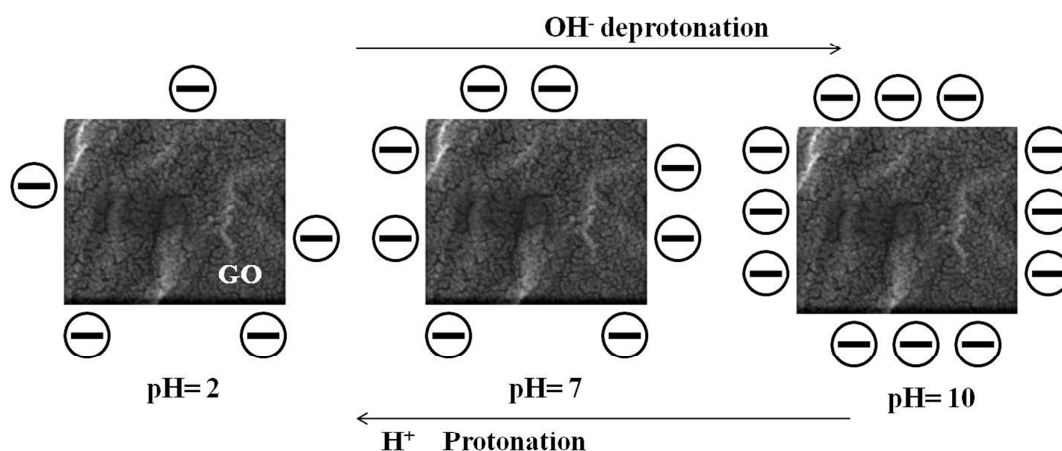


Fig. 9 Schematic representation of GO protonation and deprotonation at acidic and basic pH respectively

Discussion

Though the binding and rejection mechanisms are not completely clear at atomic level, there are certain factors which directly or indirectly affect the whole filtration process. In our studies, standard BSA concentration was used but increase in BSA concentration increases the binding and rejection capabilities of the membranes till a saturation point [55]. Other parameter is the temperature which affects certain proteins and dyes. In the case of RO-16 the removal is favoured at lower temperatures [57].

One of the most important parameter that has to be addressed is the advantage of using different concentrations of GO in the whole process. As shown in the above mentioned data it can be clearly seen that GO-PSf composite membranes produce far better results than bare PSf membranes. If GO was not used as an intermediate the mechanical strength, contact angle, pore size, surface charge, roughness, Young's modulus and permeability will highly be altered in comparison to bare PSf membrane (Table 1).

UV spectroscopy results suggest that the binding between bare PSf membranes and BSA was negligible in comparison to PSf-GO. BSA coated membranes fared better in terms of dye filtration, which means that GO is creating an internal platform for BSA binding. The relation between size and surface charge of BSA molecules and GO plays an important role in increasing the BSA binding efficiency which in turn increases the dye rejection capability.

The chemical structure and property of BSA to bind to both GO and RO-16 (Reactive Orange) textile dye makes it feasible for dye filtration.

To understand the complete mechanism that was involved in the dye rejection process it is quite important to know the effect of pH on GO, BSA and RO-16.

Effect of pH on GO

GO sheets primarily contain hydroxyl and epoxy groups which makes it more hydrophilic [64] but recently reported studies state that small quantities of COOH groups at the edges of GO sheets are the ones which actually determine the solution behaviour of GO sheets [65,66].

According to MD simulation results it was figured out that the basal plane of GO is much hydrophobic compared to the COOH edges. It is this COOH which determines the solution behaviour of GO [66]. It has also been reported that at lower pH the COOH groups are protonated (Figure 9) and the sheets become less hydrophilic and form aggregates but do not precipitate due to the formation of GO-water-GO sandwich structure which keeps it stable and surface active [67]. However at high pH, GO sheets are more hydrophilic due to the deprotonated carboxyl groups (Figure 9) which tend to dissolve in water like salt. So these larger differences make GO behave like an amphiphile [67].

Particles with zeta potential ranging from -30mv to +30mv are considered to be stable due to the electrostatic repulsions [68,69]. Also at lower pH the zeta potential is drastically less compared to at higher pH which means that at low pH the surface negative charge is less as the carboxyl groups are highly protonated [67,68].

GO sheets at higher pH act like surfactants and also as calculated by Chih et al [65], the surface tension of GO at pH=14 is around 72 dyn/cm which also suggests that GO concentration doesn't really effect the overall film or solution properties at high pH. Interestingly at lower pH values the surface tension reduces drastically from 70 to 52 dyn/cm with increase in GO concentration which shows that GO sheets are surface active at lower pH.

Though our experiments are related to GO composite membranes it is also important to understand the behaviour of GO sheets in a solution. An interesting fact to know regarding the effect of pH on the sheet size of GO is that with increase in pH the sheet size and stability increases. Swarnima et al. has explained this phenomenon [68] by DLS (Dynamic Light Scattering) technique. Generally, to increase the pH, NaOH is used (also in our case) which acts as a hydrogenating agent for GO [70]. On the other hand when HCl is used to reduce the pH, very large graphene oxide sheets with poor stability are observed. This can be attributed to the increase in H^+ ion concentration within the solution which gradually increases the sheet size [66] (increase in H^+ ions also adds to the protonation which means the decrease in electrostatic repulsion) and in turn attracting more BSA and dye molecules to bind to the membrane.

Though the surface charge and contact angle decrease with the increase of protonation at lower pH, the degree of change varies from dispersed GO to integrated GO. El kadi et al's [71] work gives more insight in to this where supernatant GO (SGO) and remanent GO (RGO) were compared at different pH values. Overall, the degree of change in terms of protonation, surface charge, contact angle and stability is in the order of SGO>RGO>composite membranes.

Effect of pH on BSA

Bovine serum albumin (BSA) undergoes conformational changes when the pH is altered from neutral to 2 [72,73] though these changes are not yet known at atomic resolution. There is a partial unfolding of the protein [74,75] and decrease in the ellipticity losing approx 40% of its initial helix [71]. The isoelectric point of BSA is 4.8 and below this value several structural alterations are caused due to the repulsive forces acting below the isoelectric point. By exposure to acid environment partial unfolding of BSA helices start, [76-78] leading to progressively exposing the protein surface to the acid environment. This leads to the increase in hydration where more and more H⁺ ions are accommodated thus leading to protonation [71]. In other words, under acidic conditions ionizable groups on BSA are protonated and due to charge repulsion, unfolding takes place [79]. Due to the protonation, BSA molecules tend to attract more dye molecules which carry surface negative charge. The higher the protonation, higher is the dye binding to BSA molecules.

At pH=7, BSA is relatively stable irrespective of the concentration and ionic strength [80].

What happens to BSA during incubation at pH=2 and pH=10?

At pH=2, BSA loses its monomers and starts to form aggregates (this is contact time dependent) which was not observed in our case as our BSA concentration and contact times are quite low (there might be a chance of formation of non-native aggregates which were undetectable).

At alkaline pH, there are certain conformational changes in BSA transforming from one form to another [81] but at high alkalinity (pH above 12) the secondary structure of BSA is completely lost [82].

The rate of degradation depends on the BSA concentration in the solution. The higher the concentration the faster is the degradation. In comparison to the study by Estey et al [80] which is related to the pH dependent degradation of BSA with time, in our case we presume that the degradation of BSA is quite low. Estey et al concluded that 100 mg/ml of BSA loses 50% of the monomers in one day which is equal to 10 mg/ml in 5 days. Considering our BSA concentration which is 100 mg/1000 ml, the degradation rate at pH=2 is calculated to be 0.05%.

Effect of pH on RO-16

Due to the presence of sulfonate groups, reactive dyes generally tend to ionize in aqueous solutions to form anions. This happens by the dissociation of sulfonate (-SO₃⁻) groups and posses negative charge. When the pH of the system decreases, it's been protonated due to the transfer of H⁺ ions, creating more binding sites and can easily attract more negatively charged dye molecules [57,83].

When the pH of the system is increased, deprotonation takes place which means more surface negative charge further resulting in electrostatic repulsion between the anionic dye molecules and negatively charged sites of the system due to which the sorption of the dye molecules at alkaline pH is less compared to acidic conditions.

Contradicting the above theory, in the experimental results presented above, the highest dye rejection value of 78.26% (before contact time studies) was observed with 2% GO membrane at pH=10 followed by 74.16% with 2% GO membrane at pH=2. Though there is a very little difference between the values, we attribute that this is because of the *Effect of initial concentration*.

Contact time study results are in correlation with the literature where there is an increase in dye rejection from 78.26% (pH=10) and 74.16% (pH=2) to 87.14% (pH=2) with 2% GO membrane. Due to the increase in contact time between BSA and dye molecules, the anionic dye molecules tend to occupy most of the available binding sites within the acidic system.

Conclusions

Protein mediated textile dye filtration using GO-PSf composite membranes has been studied and presented with experimental evidence. GO integrated polysulfone membranes were fabricated and characterized. Effect of GO concentration on protein binding and dye rejection capabilities at acidic and basic pH was experimentally elucidated.

It was observed that 2% GO membrane at pH=10 is optimal in terms of BSA binding and dye rejection capabilities. Considering the fact that RO-16 is acidic friendly, contact time studies were carried out where the BSA and dye molecules were left in contact for different time intervals (45, 90 and 135 min) before acquiring flux profile. Highest dye rejection rate observed was 87.4% (table 3) after 45 min. Higher contact times (more than 45 min) didn't render any significant advantage.

Realizing these parameters helps in developing a new class of composite membranes where the pore size more or less becomes irrelevant and will highly be dependent on binding and adsorption properties.

Acknowledgements

The authors would like to thank EC-Marie Curie Co-fund Circulation Scheme and TUBITAK (project no. 114C032) for providing financial support. We would like to extend our special thanks to Reyhan Sengur, Serkan Güçlü, Recep Kaya and Yusuf Keskin from Prof.Dr.Dincer Topacık National Membrane Research Center (MEM-TEK) at ITU for rendering their help in characterizing the membrane samples and Merve Senem Avaz from Faculty of Engineering and Natural Sciences, Sabanci University, Istanbul, for FTIR data acquisition.

References

- 1 Sangil Kim, Francesco Fornasiero, Hyung Gyu Park, Jung Bin In, Eric Meshot, Gabriel Giraldo, Michael Stadermann, Michael Fireman, Jerry Shan, Costas P. Grigoropoulos and Olga Bakajin, *J. Membr. Sci.*, 2014, **460**, 91–98.
- 2 Guangwei Li, Jing Pan, Juanjuan Han, Chen Chen, Juntao Lu and Lin Zhuang, *J. Mater. Chem. A*, 2013, **1**, 12497-12502.

- 3 Derya Y Koseoglu Imer, *Desalination*, 2013, **316**, 110-119.
- 4 Alexandra F. Bushell, Peter M. Budd, Martin P. Atfield, James T. A. Jones, Tom Hasell, Andrew I. Cooper, Paola Bernardo, Fabio Bazzarelli, Gabriele Clarizia and Johannes C. Jansen, *Angewandte Chemie*, 2013, **52**, 1253-1256.
- 5 Runhong Du, Xianshe Feng and Amit Chakma, *J. Membr. Sci.*, 2006, **279**, 76-85.
- 6 A.M. Alsamani Salih, Chunhai Yi, Jiayang Hu, Lijuan Yin and Bolun Yang, *J. Appl. Polym. Sci.*, 2014, **131**.
- 7 Derya Y. Köseoglu, Borte Kose, Mahmut Altinbas and İsmail Koyuncu, *J. Membr. Sci.*, 2012, **428**, 620-628.
- 8 K.S. Novoselov, A. K. Geim, S. V. Morozov, D. Jiang, Y. Zhang, S. V. Dubonos, I. V. Grigorieva and A.A. Firsov, *Science*, 2004, **306**, 666.
- 9 A.K. Geim and K.S. Novoselov, *Nat. Mater.*, 2007, **6**, 183.
- 10 N.M. Gabor, Justin C.W. Song, Qiong Ma, Nityan L. Nair, Thiti Taychatanapat, Kenji Watanabe, Takashi Taniguchi, Leonid S. Levitov and Pablo Jarillo-Herrero, *Science*, 2011, **334**, 648.
- 11 A.K.M. Newaz, D.A. Markov, D. Prasai and K.I. Bolotin, *Nano Lett.*, 2012, **12**, 2931.
- 12 C. Lee, X. Wei, J.W. Kysar and J. Hone, *Science*, 2008, **321**, 385.
- 13 Keun Soo Kim, Yue Zhao, Houk Jang, Sang Yoon Lee, Jong Min Kim, Kwang S. Kim, Jong-Hyun Ahn, Philip Kim, Jae-Young Choi and Byung Hee Hong, *Nature*, 2009, **457**, 706.
- 14 L. Gomez De Arco, Yi Zhang, Cody W. Schlenker, Kounghmin Ryu, Mark E. Thompson and Chongwu Zhou, *ACS Nano*, 2010, **4**, 2865.
- 15 Bae Sukang, Kim Hyeongkeun, Lee Youngbin, Xu Xiangfan, Park Jae-Sung, Zheng Yi, Balakrishnan Jayakumar, Lei Tian, Ri Kim Hye, Song Young Il, Kim Young-Jin, Kim Kwang S, Özyilmaz Barbaros, Ahn Jong-Hyun, Hong Byung Hee and Iijima Sumio, *Nat. Nano.*, 2010, **5**, 574.
- 16 N. Tsuyoshi and M. Yoshiaki, *Carbon*, 1994, **32**, 469-475.
- 17 G.I. Titelman, V.Gelman, S.Bron, R.L. Khalfin, Y.Cohen and H.Bianco-Peled, *Carbon*, 2005, **43**, 641-649.
- 18 H. Masukazu, G. Takuya, H. Shigeo, F. Masahiro and O. Michio, *Carbon*, 2004, **42**, 2929-2937.
- 19 William S. Hummers and Richard E. Offeman, *J. Am. Chem. Soc.*, 1958, **80**, 1339-1339.
- 20 Haiyang Zhao, Liguang Wu, Zhijun Zhou, Lin Zhang and Huanlin Chen, *Phys. Chem. Chem. Phys.*, 2013, **15**, 9084.
- 21 Chuanqi Zhao, Xiaochen Xu, Jie Chen and Fenglin Yang, *J. Environ. Chem. Eng.*, 2013, **1**, 349-354.
- 22 Sirius Zinadini, Ali Akbar Zinatizadeh, Masoud Rahimi, Vahid Vatanpour and Hadis Zangeneh, *J. Membr. Sci.*, 2014, **453**, 292-301.
- 23 Fengmin Jin, Wei Lv, Chen Zhang, Zhengjie Li, Rongxin Su, Wei Qi, Quan-Hong Yang and Zhimin He, *RSC Adv.*, 2013, **3**, 21394-21397.
- 24 Mariana Ionita, Andrea Madalina Pandeale, Livia Crica and Luisa Pilan, *Composites: part B*, 2014, **59**, 133-139.
- 25 Denisa Fica, Anton Fica, Georgeta Voicu, Bogdan Stefan Vaasile, Cornelia Guran and Ecaterina Andronescu, *Mater Plast.*, 2010, **47**.
- 26 S.I. Voicu, M.A. Pandeale, E. Vasile, R. Rughinis, L. Crica, L. Pilan and M. Ionita, *Dig. J. Nanomater. Bios.*, 2013, **8**, 1389-1394.
- 27 Jiguo Zhang, Zhiwei Xu, Mingjing shan, Baoming Zhou, Yinglin Li, Baodong Li, Jiarong Niu and Xiaoming Qian, *J. Membr. Sci.*, 2013, **448**, 81-92.
- 28 Jaewoo Lee, Hee-Ro Chae, Young June Won, Kibaek Lee, Chung-Hak Lee, Hong H. Lee, In-Chul Kim and Jong Min Lee, *J. Membr. Sci.*, 2013, **448**, 223-230.
- 29 Chuanqi Zhao, Xiaochen Xu, Jie Chen, Guowen Wang and Fenglin Yang, *Desalination*, 2014, **340**, 59-66.
- 30 B.M. Ganesh, Arun M. Isloor and A.F. Ismail, *Desalination*, 2013, **313**, 199-207.
- 31 Swati Gahlot, Prem P. Sharma, Hariom Gupta, Vaibhav Kulshrestha and Prafulla K. Jha, *RSC Adv.*, 2014, **4**, 24662-24670.
- 32 Jianfeng Shen, Min Shi, Bo Yan, Hongwei Ma, Na Li, Yizhe Hu and Mingxin Ye, *Colloids Surf B.*, 2010, **81**, 434-438.
- 33 Xiujuan Xu, Jing Huang, Jijun Li, Jiawei Yan, Jingui Qin and Zhen Li, *Chem. Commun.*, 2011, **47**, 12385-12387.
- 34 B.G. Choi, H.S. Park, T.J. Park, M.H. Yang, J.S. Kim and S.Y. Jang, *ACS Nano*, 2010, **4**, 2910.
- 35 Hikaru Tateishi, Kazuto Hatakeyama, Chikako Ogata, Kengo Gezuhara, Jun Kuroda, Asami Funatsu, Michio Koinuma, Takaaki Taniguchi, Shinya Hayami and Yasumichi Matsumoto, *J. Electrochem. Soc.*, 2013, **160**, F1175-F1178.
- 36 D. Chen, H. Feng and J. Li, *Chem. Rev.*, 2012, **112**, 6027.
- 37 S.Y. Wong, Y.P. Tan, A.H. Abdullah and S.T. Ong, *MJAS*, 2009, **13**, 185-193.
- 38 R. Gong, Y. Sun, J. Chen, H. Liu and C. Yang, *Dyes Pigments.*, 2005, **67**, 175-181.
- 39 V. Fu and T. Viraraghava, *Water SA.*, 2003, **29**, 465.
- 40 P.K.Gill, D.S.Arora and M.Chander, *J. Ind. Microbiol. Biot.*, 2002, **28**, 201.
- 41 Sung Wook Won, Hyung Joong Yun and Yeoung-Sang Yun, *J. Colloid Interface Sci.*, 2009, **331**, 83-89.
- 42 Madhuri M. Sahasrabudhe and Girish R. Pathade, *Eur. J. Exp. Biol.*, 2011, **1**, 163-173.
- 43 Sidra Ilyas and Abdul Rehman, *Iranian J. Environ. Health Sci. Eng.*, 2013, **10**:12, doi:10.1186/1735-2746-10-12.
- 44 Gang Fan, Jianlong Ge, Hak-Yong Kim, Bin Ding, Salem S. Al-Deyab, Mohamed El-Newehy and Jianyong Yu, *RSC Adv.*, 2015, **5**, 64318-64325.
- 45 Ajith Pattammattel, Megan Puglia, Subhrakanti Chakraborty, Inoka K. Deshapriya, Prabir K. Dutta and Challa V. Kumar, *Langmuir*, 2013, **29**, 15643-15654.
- 46 C. Zhao, X. Xu, J. Chen, G. Wang and F. Yang, *Desalination*, 2014, **340**, 59-66.
- 47 K. Hu, D.D. Kulkarni, I. Choi and V.V. Tsukruk, *Prog. Polym. Sci.*, 2014, **39**, 1934-1972.
- 48 H. Strathmann and K. Kock, *Desalination*, 1977, **21**, 241-255.
- 49 M. Cheryan, *Ultrafiltration and Microfiltration handbook*, CRC Press, Lancaster, USA, 1998.
- 50 H. Wu, B. Tang and P. Wu, *J Membr Sci.*, 2010, **362**, 374-83.
- 51 J. Shen, M. Shi, B. Yan, H. Ma, N. Li, Y. Hu and M. Ye, *Colloids Surf. B Biointerfaces*, 2010, **81**, 434-8.
- 52 Theodore Peters, Jr. *All About Albumin: Biochemistry, Genetics*, ISBN: 978-0-12-552110-9, 1995.
- 53 M. Dockal, D.C. Carter and F. Ruker, *J. Biol. Chem.*, 2000, **275**, 3042.
- 54 V.M. Rosenoer, M. Oratz and M.A. Rothschild, *Permagon press*, NY, 1977, 53-84.
- 55 J. Sereikaite, Z. Bumeliene and V.A. Bumelis, *Acta Chromatographica*, 2005, **15**.
- 56 Ute Bohme and Ulrich Scheler, *Chem. Phys. Lett.*, 2007, **435**, 342-345.
- 57 S.Y. Wong, Y.P. Tan, A.H. Abdullah and S.T. Ong, *J. Phys. Sci.*, 2009, **20**, 59-74.
- 58 M. Ozacar and I.A. Sengil, *J. Hazard. Mater. B*, 2003, **98**, 211-224.
- 59 M.S. Chiou and H.Y. Li, *Chemosphere*, 2003, **50**, 1095-1105.
- 60 T. Ohashi, A.M. Jara, A.C. Batista, L.O. Franco, M.A. Barbosa Lima, M. Benachour, C.A. Alves da Silva and G.M. Campos-Takaki, *Molecules*, 2012, **17**, 14219-14229.
- 61 N. Holm, *Biochim. Biophys. Acta*, 2007, **1774**, 1128-1138.
- 62 D. Gao, Y. Tian, F. Liang, D. Jim, Y. Chen, H. Zhang and A. Yu, *J. Lumin.*, 2007, **127**, 515-522.
- 63 K.G. Bhattacharyya and A. Sharma, *Dyes Pigments.*, 2003, **57**, 211-222.

- 64 S. Stankovich, D.A. Dikin, R.D. Piner, K.A. Kohlhaas, A. Kleinhammes, Y. Jia, Y. Wu, S.T. Nguyen and R.S. Ruoff, *Carbon*, 2007, **45**, 1558–1565.
- 65 A. Lerf, A.H.Y. He, M. Forster and J. Klinowski, *J. Phys. Chem. B*, 1998, **102**, 4477–4482.
- 66 X.L. Li, G.Y. Zhang, X.D. Bai, X.M. Sun, X.R. Wang, E. Wang and H.J. Dai, *Nat. Nanotechnol.*, 2008, **3**, 538–542.
- 67 Chih-Jen Shih, Shangchao Lin, Richa Sharma, Michael S. Strano and Daniel Blankschtein, *Langmuir*, 2012, **28**, 235–241.
- 68 Swarnima Kashyap, Shashank Mishra and Shantanu K. Behera, *Journal of Nanoparticles*, 2014, ID 640281.
- 69 R.J. Hunter, *Foundations of colloid science*, 2001, **2**, 376–377 Oxford University Press.
- 70 T. Kulia, P. Khanra, N.H. Kim, J.K. Lim and J.H. Lee, *J. Mat. Chem. A*, 2013, **1**, 9294–9302.
- 71 N. El Kadi, N. taulierm J.Y. Le Huerou, M. Gindre, W. Urbach, I. Nwigwe, P.C. Kahn and M. Waks, *Biophys. J.*, 2006, **91**, 3397–3404.
- 72 J.F. Foster, Plasma albumin, In the plasma proteins, 1960, Academic Press, New York, 179–239.
- 73 J.F. Foster, Binding properties of albumin, In Albumin Structure, Function and Uses, 1977, Pergamon Press, Oxford, 53–84.
- 74 T.J. Peters, Serum albumin, *Adv. Protein. Chem.*, Academic Press, New York, 1985, 161–245.
- 75 C.D. Carter and J.X. Ho, Structure of serum albumin, *Adv. Protein. Chem.*, Academic Press, New York, 1994, 153–203.
- 76 K. Foygel, S. Spector, S. Chatterjee and P.C. Kahn, *Protein Sci.*, 1995, **4**, 1426–1429.
- 77 M.D. Dockal, C. Carter and F. Ruker, *J. Biol. Chem.*, 2000, **275**, 3042–3050.
- 78 K. J. Frye and C. Royer, *Protein Sci.*, 1998, **7**, 2217–2222.
- 79 C. Tanford, *Adv. Protein. Chem.*, 1968, **23**, 131–282.
- 80 Tia Estey, Jichao Kang, Steven P. Schwendeman and John F. Carpenter, *Journal of Pharmaceutical Sciences*, 2006, **95**, 1626–1639.
- 81 Peter J. Sadler and Alan Tucker, *Eur. J. Biochem.*, 1993, **212**, 811–817.
- 82 B. Ahmad, M.Z. Kamal and R.H. Khan, *Protein. Pept. Lett.*, 2004, **11**, 307–315.
- 83 M.S. Chiou and H.Y. Li, *Chemosphere*, 2003, **50**, 1095–1105.